Journal of Power Sources 185 (2008) 1334–1339

Contents lists available at ScienceDirect

Journal of Power Sources

journal homepage: www.elsevier.com/locate/jpowsour

Hydrogen generation from hydrides in millimeter scale reactors for micro proton exchange membrane fuel cell applications

L. Zhu[a,*], D. Kim[c], H. Kim[b], R.I. Masel[b], M.A. Shannon[a]

[a] Department of Mechanical Science and Engineering, University of Illinois at Urbana Champaign, 1206 West Green Street, Urbana, IL 61801, USA
[b] Department of Chemical and Biomolecular Engineering, University of Illinois at Urbana Champaign, 600 South Mathews Avenue, Urbana, IL 61801, USA
[c] Department of Mechanical Engineering, Sogang University, 1 Shinsu-dong, Mapo-gu, Seoul, Republic of Korea

ARTICLE INFO

Article history:
Received 14 July 2008
Received in revised form 26 August 2008
Accepted 26 August 2008
Available online 7 September 2008

Keywords:
Hydrogen generation
Micro reactor
Micro-PEM fuel cell
Hydride
Hydrolysis reaction

ABSTRACT

This paper introduces and discusses the feasibility of millimeter scale powder packed-bed reactors using high energy density chemical hydrides for micro-PEM fuel cell applications. Two different reactors were designed and tested using $LiBH_4$, $LiAlH_4$, $NaAlH_4$ and CaH_2 hydride fuels. The mechanisms that limit the total yield of H_2 generated and impact the performance of the hydrogen generator are investigated in this paper, including density, solubility and porosity of the reaction byproducts. The volume expansion of the byproducts has significant effect on the total energy density of micro-hydrogen generators because the byproducts are left in the millimeter scale reactor after the reactions and the micro-hydrogen generators have limited fuel storage space. The SEM images of the reaction byproducts indicates that the byproducts of $LiBH_4$ can form a single solid mass that clogged the reaction vessel and limit the full utilization of the hydride. However, the byproducts of $LiAlH_4$ and CaH_2 reactions are non-agglomerated and they do not form impermeable mass. The experimental results show that the highest yield of hydrogen generation was achieved with $LiAlH_4$ and CaH_2 fuels.

1. Introduction

Proton exchange membrane (PEM) fuel cells have attracted considerable attention as small power sources for portable electronic devices due to its relatively high power density, environmental friendly products, and simple and rapid recharging [1–4]. Most of the current research work is focused on the development of portable PEM fuel cells that meet the demand of portable electronic devices with 1–10 W electric power [5–22]. However, sub-millimeter power sources are also needed for micro sensors, cognitive arthropods, subdermal drug delivery systems, and other applications. Generally, the devices require peak power levels above one milliwatt, and have mission durations of an hour to a few days. To this end, only a few studies have been performed in this area [23–29], but none of them include the microscale on-board fuel storage system.

In order to meet the energy density requirements for microscale power sources, the volumetric energy density of fuels is a critical target, due to constraints on fuel storage space. Compared with hydrocarbon fuels such as methanol and formic acid, hydrogen generation from metal and chemical hydrides shows the potential of being used in micro-fuel cell applications due to its high energy density. As shown in Fig. 1, metal and chemical hydrides such as sodium borohydride ($NaBH_4$) [30–32], lithium borohydride ($LiBH_4$) [33,34], lithium aluminum hydride ($LiAlH_4$) [35], sodium aluminum hydride ($NaAlH_4$) [35] and calcium hydride (CaH_2) [35,36] have relatively high theoretical hydrogen volumetric density [37,38]. To this end, several approaches have been explored to build hydrogen generators for portable fuel cells, but the sub-millimeter hydrogen generators still remain an unsolved problem. The objective of this literature review [3,35–49] is to investigate whether the current approaches for portable power sources can be accepted for the micro-power source applications. As shown in the literatures, the catalyst packed-bed reactor using a catalytic hydrolysis reaction of alkaline sodium borohydride and sodium hydroxide (NaOH) solution has been widely reported [3,39–47]. However, the diluted $NaBH_4$ solution reduces the overall fuel energy density, which is not desired in micro-scale systems. Instead of using catalyst packed-bed reactors, chemical hydride powder packed-bed reactors have been designed to generate hydrogen [35,36,48,49]. A solid lithium hydride powder packed-bed reactor has been designed to characterize the kinetic behavior of the lithium hydride hydrolysis reaction on a small scale in 1996. In this design, the hydrolysis reaction of lithium hydride required 15–20 times the stoichiometric water ratio to complete the reaction and remove the byproduct (LiOH) from the reaction site. The excess water can significantly

* Corresponding author. Tel.: +1 217 244 7301; fax: +1 217 244 6534.
E-mail address: lzhu@uiuc.edu (L. Zhu).

0378-7753/$ – see front matter © 2008 Elsevier B.V. All rights reserved.
doi:10.1016/j.jpowsour.2008.08.092

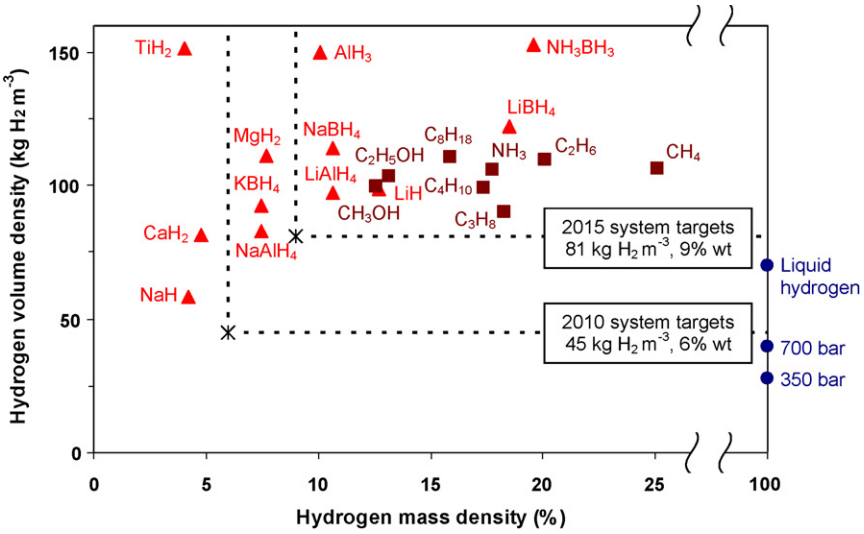

Fig. 1. A regime map of various hydrogen densities for different materials containing hydrogen [37] and U.S. Department of Energy's Freedom Car Program targets for 2010 and 2015 [38]. The values shown assume complete conversion of the hydride itself into hydrogen.

decrease the energy density of the on-board hydrogen generation system, if a water recycling system is not employed, because the excess water has no energy content. As shown in Kong et al.'s work [36], nickel mesh basket was used to contain hydride powders in the reactor and liquid water was added to the bottom of the reaction vessel. However, the volume of the nickel mesh basket is about 3% of the volume of the whole device, and the energy density of the whole device is significantly decreased.

This study focuses on millimeter scale metal or chemical hydrides powder packed-bed reactors using pure water for use in micro-hydrogen PEM fuel cells. Compared with large scale hydride powder packed-bed reactors, millimeter scale reactors need to efficiently pack hydride powders to achieve high energy density due to constraints on fuel storage space. However, the volume expansion of the byproducts is a tradeoff in the microscale design. The reaction chamber cannot be filled with solid fuels completely, because the volume of the reaction byproducts left in the reactor after the reactions is always larger than the volume of the solid fuels. More hydride loading has the potential of generating more hydrogen; on the other hand, more hydride loading leaves less space for volume expansion which can cause the reaction vessel to clog or break. Ideally, the spare space in the reactor should be equal to the volume expansion of total hydride reaction. The properties of the byproducts, such as density, solubility, and porosity, are studied in this paper because the byproducts limit the total yield of H_2 generated and impact the performance of the hydrogen generator. If the byproducts form impermeable materials, the reaction vessel can become clogged and the chemical hydride on the output side remains unreacted, which can cause significant hydrogen yield losses, and thus a decrease in the maximum energy density possible. The density and porosity of the byproducts directly determine the volume utilization efficiency of the reaction chambers.

In the present work, two chemical hydride powder packed-bed reactors with sub-mL reaction vessel were designed and tested using $LiBH_4$, $LiAlH_4$, $NaAlH_4$ and CaH_2 hydride fuels. The hydrogen generation yield of the reactor was measured, and the hydrogen volume density was calculated based on the yield. The purpose of this study is to present the yield and hydrogen volume density results found in the reactors, and to elucidate the mechanisms that limit the yields and hydrogen volume densities. The paper first presents a description of the experimental techniques used to measure the yield of hydrogen generation with the hydride powder packed-bed reactors. Next, the hydrogen generation results for $LiBH_4$, $LiAlH_4$, $NaAlH_4$ and CaH_2 are presented. The properties of the byproduct of all the hydrides, such as porosity and solubility, are presented, and the mechanisms that limit the hydrogen generation yields are discussed. Finally a CaH_2 powder packed-bed reactor was connected to a micro-silicon fuel cell, the performance of the system, such as polarization curve and power density plot was presented.

2. Experimental

2.1. Apparatus

A schematic of the experimental setup used to measure the hydrogen generation is shown in Fig. 2. The apparatus consisted of a small scale reactor, a syringe pump (Harvard Apparatus, Holliston, MA), and a water trap to measure the volume of generated hydrogen. Two different reactors were used in this experiment, and both were made of Teflon. Reactor 1 was sealed by two plugs with water inlet plug having a central hole covered with a porous glass filter and another hydrogen outlet plug having a central hole covered with a porous polyethylene filter. The two plugs were at the two ends of the reaction vessel, and the volume of the reaction ves-

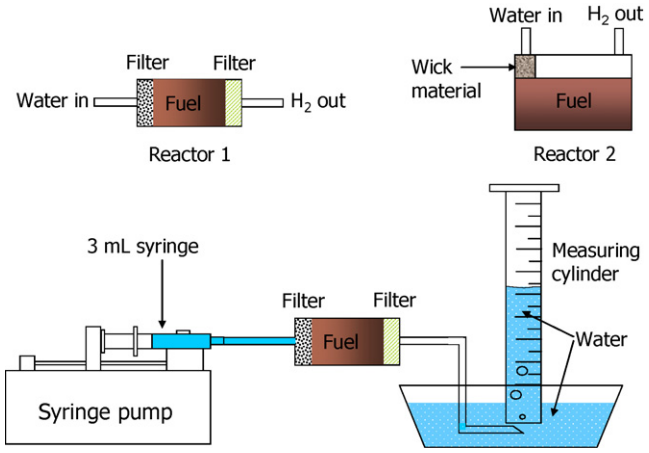

Fig. 2. Schematic of the experimental setup. Both reactors are made of Teflon, with inner volume of 56 μL and 200 μL, respectively.

Table 1
Hydrogen volumetric density of some hydrogen generation reactions

Hydrolysis reactions	Hydrogen generation (hydrogen/reactants) ($mm^3\ mm^{-3}$)	Volume expansion (byproducts/hydride) (%)	Hydrogen generation with volume expansion (hydrogen/reactants) ($mm^3\ mm^{-3}$)
$AlH_3 + 3H_2O \rightarrow Al(OH)_3 + 3H_2$ [50]	988	161	848
$LiBH_4 + 4H_2O \rightarrow H_3BO_3 + LiOH + 4H_2$ [51]	934	178	747
$NaBH_4 + 4H_2O \rightarrow H_3BO_3 + NaOH + 4H_2$ [51]	912	173	734
$NaBH_4 + 3H_2O + HCl \rightarrow H_3BO_3 + NaCl + 4H_2$ [52]	905	197	675
$MgH_2 + 2H_2O \rightarrow Mg(OH)_2 + 2H_2$ [50]	902	134	801
$LiH + H_2O \rightarrow LiOH + H_2$ [51]	882	286	530
$LiAlH_4 + 4H_2O \rightarrow Al(OH)_3 + LiOH + 4H_2$ [51]	863	117	815
$NaAlH_4 + 4H_2O \rightarrow Al(OH)_3 + NaOH + 4H_2$ [50]	846	118	788
$CaH_2 + 2H_2O \rightarrow Ca(OH)_2 + 2H_2$ [36]	843	150	706

sel is 56 μL. Reactor 2 was sealed by three plugs and the volume of the reaction vessel is 200 μL. Two plugs with a central hole were at one end of the reaction vessel for water and hydrogen flow. Another plug was used to seal the reaction vessel after loading the hydrides powder. At the water inlet port, a small piece of polyester membrane was used as a wicking material. The syringe pump was used to deliver water into the reaction vessel to react with the hydrides. As shown in Fig. 2, water was introduced through the plug on the left and the hydrogen was taken out through the plug on the right. The generated hydrogen gas was collected and its volume was measured in the water trap, which consisted of an inverted, water-filled 100 mL graduated cylinder immersed in a water-filled tray, and interconnected with the reactor by PVC tubing.

2.2. Materials

The calcium hydride, lithium aluminum hydride, and sodium aluminum hydride were purchased from Aldrich chemical company (St. Louis, MO). Lithium borohydride was purchased from Fisher Scientific Company (Fair Lawn, New Jersey). Water used in this experiment was from Millipore Direct-Q™ 5 Ultrapure Water Systems bought from Fisher Scientific Company.

2.3. Procedures

Since the hydrides can react with the moist air to liberate hydrogen, the hydrides samples were weighed and loaded into the reactor inside a glove box (Innovative Technology, Newburyport, MA), which was purged and inflated with dry nitrogen gas. All the experiments were conducted at room temperature of 25 °C and the local heating caused by the exothermic reaction was neglected. The experiments were conducted with four hydrides, $LiBH_4$, $LiAlH_4$, $NaAlH_4$ and CaH_2. Millipore water (18.2 MOhm-cm water) was the only liquid reactants used in this study. In order to control the rate of hydrogen production, the Millipore water was loaded into a Becton Dickinson (BD) 3 mL plastic syringe and introduced into the reactor by the syringe pump at a flow rate of 10 $\mu L\ h^{-1}$. The hydrogen gas was collected and measured in a water trap.

3. Results and discussion

There are lots of commercial available hydrides which can be used to generate hydrogen. As shown in the literatures, hydrogen generation results from the hydrolysis reactions shown in Table 1 [36,50–52]. In this work, four hydrides, $LiBH_4$, $LiAlH_4$, $NaAlH_4$ and CaH_2, were studied, because they have faster and more complete hydrolysis reaction with pure water. The experimental hydrogen yield is calculated from the measured hydrogen volume over the theoretical hydrogen volume. The hydrogen generation stops due to completion of the reaction or the reaction vessel clog, preventing complete reaction. In addition, liquid solution can flow out of the reactor due to a low reaction rate or high water flow rate. The byproduct solution can contaminate the proton exchange membrane of the fuel cell because the anode of the fuel cell will be directly connected to the hydrogen generator. In this case, the experimental hydrogen yield is calculated by the measured hydrogen volume over the theoretical hydrogen volume when byproduct solution flows out of the reactor.

In order to control the hydrogen generation rate, a syringe pump is used to deliver water to the reactor at a flow rate of 10 $\mu L\ h^{-1}$. The stoichiometric amount of water is delivered to the hydrides to complete hydrolysis reaction and achieve maximum hydrogen volumetric density. The hydrogen generation profiles for $LiAlH_4$ and CaH_2 with two reactors are shown in Fig. 3, and the results are summarized in Table 2. The syringe pump stopped pumping water into the reactor when stoichiometric amount of water was delivered to the hydrides. As shown in Fig. 3a, both $LiAlH_4$ and CaH_2 can reach 80% yield with Reactor 1, and 90% yield with Reactor 2. A 100% yield is achieved within several hours after stopping pumping. All the reactions can give an almost constant hydrogen generation rate from 10% yield to the point that stoichiometric amounts of water is delivered to the reactor, denoted by large circle, triangle, diamond, and square points in Fig. 3a. Because the hydrides powders are very hygroscopic and they can absorb water at the beginning, the initial hydrogen generation rate is higher than the constant rate. As shown in Fig. 3b, the hydrogen generation rates are almost the same in the constant hydrogen generation region. According to the reac-

Table 2
Summary of hydrogen generation results for CaH_2 and $LiAlH_4$ using Reactor 1 and Reactor 2

	CaH_2 (≥97%)		$LiAlH_4$ (≥95%)	
	Reactor 1	Reactor 2	Reactor 1	Reactor 2
Weight of hydride (mg)	51	92.7	16.8	33.6
Water (μL)	42.3	76.9	30.2	60.6
Hydrogen (mL)	57.3	104.4	36.9	82
Volume of the reactor (μL)	56	200	56	200
Yield (%)	99.7	99.8	89.8	99.6
Volume density (mm^3 H_2 per mm^3 of reactants)	828.7	830.6	761.4	844.3
Volume density with byproducts volume expansion (mm^3 H_2 per mm^3 of reactants)	695.9	698.0	714.6	792.5

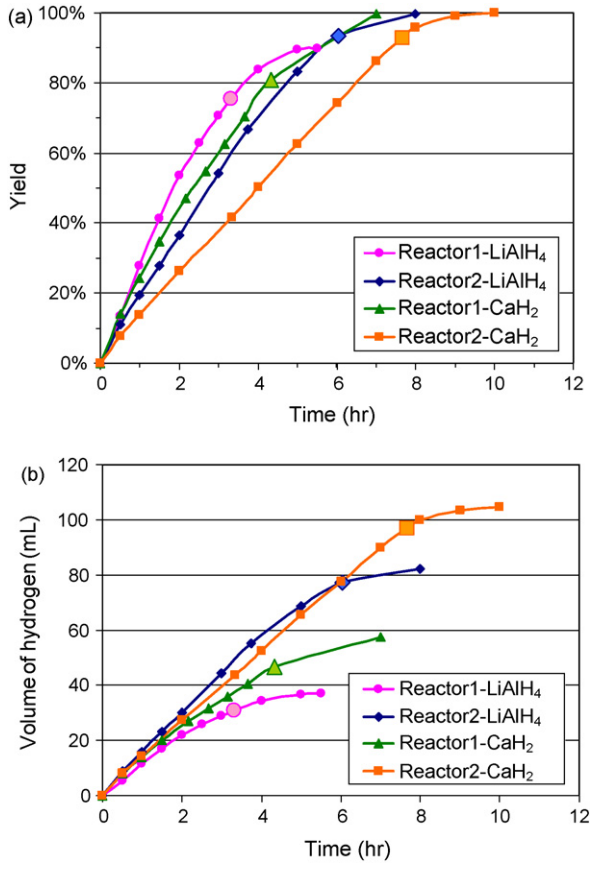

Fig. 3. Hydrogen generation profile of (a) yield and (b) volume of generated hydrogen for the hydrolysis reactions of CaH_2 and $LiAlH_4$. Water was delivered to the reactor by a syringe pump at 10 μL h^{-1}. Large circle, triangle, diamond, and square points denote the points that stoichiometric amounts of water was delivered to the reactor.

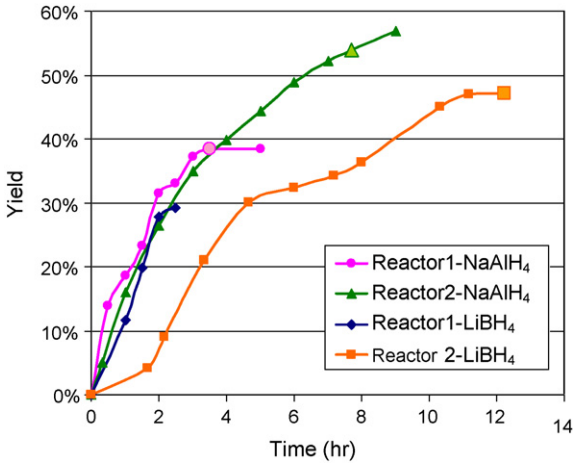

Fig. 4. Hydrogen generation profile for the hydrolysis reactions of $LiBH_4$ and $NaAlH_4$. Water was delivered to the reactor by a syringe pump at 10 μL h^{-1}. Large circle, triangle, diamond, and square points denote the points that stoichiometric amounts of water was delivered to the reactor. Reactor 1 with $LiBH_4$ did not use stoichiometric amount of water, because the reaction vessel was clogged before the points that stoichiometric amounts of water was delivered to the reactor.

tion formulas of $LiBH_4$, $LiAlH_4$, $NaAlH_4$ and CaH_2 shown in Table 1, the mole number of hydrogen is equal to the mole number of water. The hydrogen generation rate is determined by the water delivering rate, if the reaction rate is much higher than the water delivery rate. In this experiment, the same water delivering rate for all the reactions, 10 μL h^{-1}, results in the same hydrogen generation rate in the constant hydrogen generation region. After stopping pumping at stoichiometric amount of water, the hydrogen generation yields are close to 100%, and the hydrogen generation rate drops off significantly. The hydrogen volumetric densities were calculated and summarized in Table 2. All the reactions have a hydrogen volumetric density higher than 750 mm^3 H_2 per mm^3 of reactants. $LiBH_4$ and $NaAlH_4$ were also tested using the same apparatus and procedures. The hydrogen generation profiles are shown in Fig. 4 and the results are summarized in Table 3. $LiBH_4$ has 29.3% hydrogen generation yield with Reactor 1 and 47.2% yield with Reactor 2. $NaAlH_4$ has 43.3% hydrogen generation yield with Reactor 1 and 55.4% yield with Reactor 2. The overall hydrogen volumetric densities of $LiBH_4$ and $NaAlH_4$ are less than that of $LiAlH_4$ and CaH_2.

As described in introduction, solubility and porosity of the reaction products can cause different fuel utilization among the four hydrides. According to the reaction formulas in Table 1, $LiAlH_4$ produces insoluble byproducts, LiOH and $Al(OH)_3$. CaH_2 produces insoluble byproduct, $Ca(OH)_2$. $LiBH_4$ produces a soluble byproduct, H_3BO_3, and an insoluble byproduct, LiOH. $NaAlH_4$ produces a soluble byproduct, NaOH, and an insoluble byproduct, $Al(OH)_3$. At present, most of the portable hydrogen generators require the byproducts to be soluble to facilitate handling and ease of use, and reduce the effort required to remove byproducts from the generator. However, the target of this research is to develop micro-hydrogen generators for micro-PEM fuel cell applications. So the final device will be disposable instead of being rechargeable, and the byproducts should be left in the reactor after completion of the reaction. In this case, insoluble byproducts are desired in the disposable micro-hydrogen generator, and the porosity of the byproducts, which determines how much water and hydrogen can diffuse through the packed-bed reactor, directly affects the hydrogen yield of the reactions in each reactor type.

We have found that the products of $LiBH_4$ reaction and unreacted $LiBH_4$ can form a single solid and impermeable mass that can clog the reaction vessel, leaving unreacted $LiBH_4$ on the output side. However, the products of $LiAlH_4$ and CaH_2 reactions do not form an impermeable mass. This point can be illustrated by the SEM images of the reaction products. In Fig. 5a, no pores can be found on the surface of the $LiBH_4$ reaction products, and Fig. 5b and c show that the products of $LiAlH_4$ and CaH_2 reactions are non-agglomerated

Table 3
Summary of hydrogen generation results for $LiBH_4$ and $NaAlH_4$ using Reactor 1 and Reactor 2

	$LiBH_4$ (≥95%)		$NaAlH_4$ (≥90%)	
	Reactor 1	Reactor 2	Reactor 1	Reactor 2
Weight of hydride (mg)	16	39	26.4	61.5
Water (μL)	25	122.5	31.7	73.8
Hydrogen (mL)	20	78.5	16.5	57
Volume of the reactor (μL)	56	200	56	200
Yield (%)	29.3	47.2	38.4	56.9
Volume density (mm^3 H_2 per mm^3 of reactants)	408	433.6	311.4	461.9

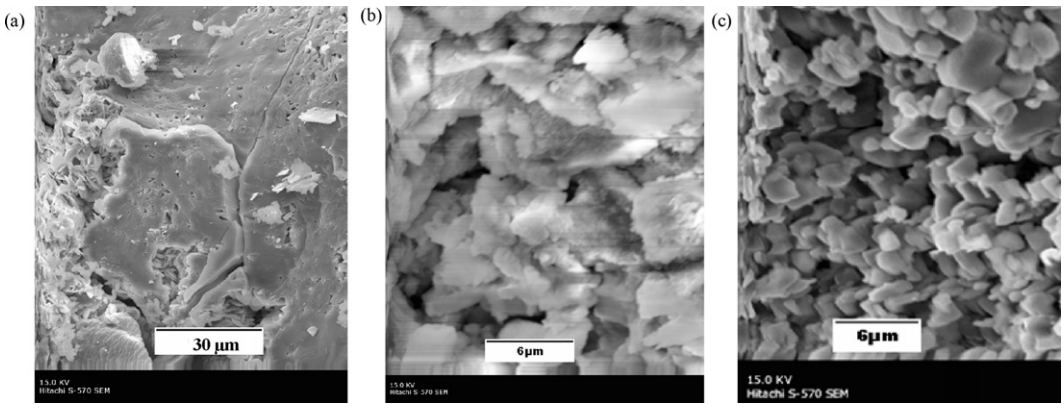

Fig. 5. SEM images of reaction products from hydrolysis reaction of (a) $LiBH_4$; (b) CaH_2; and (c) $LiAlH_4$.

and they do not form impermeable mass. The hydrolysis reaction of $NaAlH_4$ produces both soluble and insoluble byproducts, but they do not form impermeable solid mass as the byproducts of $LiBH_4$ reaction do. The byproducts of $NaAlH_4$ reaction and water form alkaline "slurry" in the hydrogen reactor, which reduces the reaction rate and results in a lower yield with stoichiometric water addition.

For the current reactor design, the byproducts of the hydrolysis reaction are left in the reactor after completion of the reaction, and the volume expansion of the byproducts has to be considered due to constraints on fuel storage space and high energy density requirement. The actual hydrogen volumetric density is related to the volume expansion rate of byproducts, which is calculated by the volume of byproducts over the volume of hydride. Theoretically the maximum actual hydrogen volumetric density for this reactor with fixed volume is calculated by the volume of generated hydrogen at room temperature and 1 atm over the total volume of water and the byproducts. As shown in Table 1, the hydrolysis reaction of lithium hydride has the largest byproducts volume expansion about 286%, which causes the lowest actual hydrogen volumetric density. Although AlH_3, $NaBH_4$, and $LiBH_4$ have higher hydrogen volumetric density than $LiAlH_4$, $NaAlH_4$, MgH_2, and CaH_2, their actual hydrogen volumetric densities are similar, because $LiAlH_4$, $NaAlH_4$, MgH_2, and CaH_2 have relatively lower byproducts volume expansion. If the byproducts volume expansion is considered, the actual hydrogen volumetric densities for $LiAlH_4$ and CaH_2 are around 700 mm^3 H_2 per mm^3 of reactants.

There are some other hydrides with higher volumetric hydrogen density shown in Table 1, which can react with pure water to generate hydrogen. However, they cannot complete the hydrolysis reaction with stoichiometric pure water. For instance, $NaBH_4$ requires catalyst or additional acid to complete the reaction, because the basic byproduct NaOH can increase the pH of the reaction solution, which slows down the reaction rate [53]. MgH_2 has a high hydrogen volumetric density, but the reaction usually stops before total completion due to the formation of passivation layers [54]. AlH_3 is another hydride with a high hydrogen volumetric density, but it does not react noticeably in pH neutral media, decomposing only 1% in more than an hour at 40 °C [50]. Additional catalyst and/or acid have to be added to achieve a faster and more complete reaction for these hydrides, which can decrease the energy density of the hydrolysis reactions and are not desired in the micro-hydrogen generators.

Finally, Reactor 1 filled with CaH_2 powder was connected to a hybrid silicon fuel cell to test the fuel cell performance with the hydrogen generated from the hydride powder packed-bed reactor. The hybrid silicon fuel cell is depicted in Fig. 6 and will be discussed in another paper. Briefly, the silicon fuel cell is fabricated from a 325 μm thick SOI wafer (25 μm thick device layer) using MEMS

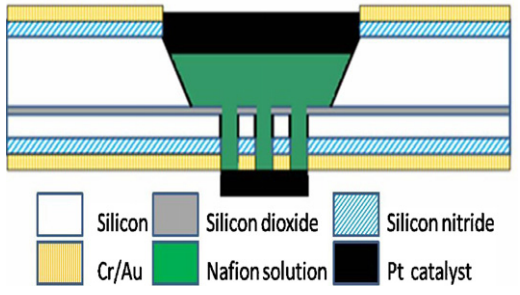

Fig. 6. Schematic of the Nafion® filled silicon fuel cell on a SOI wafer.

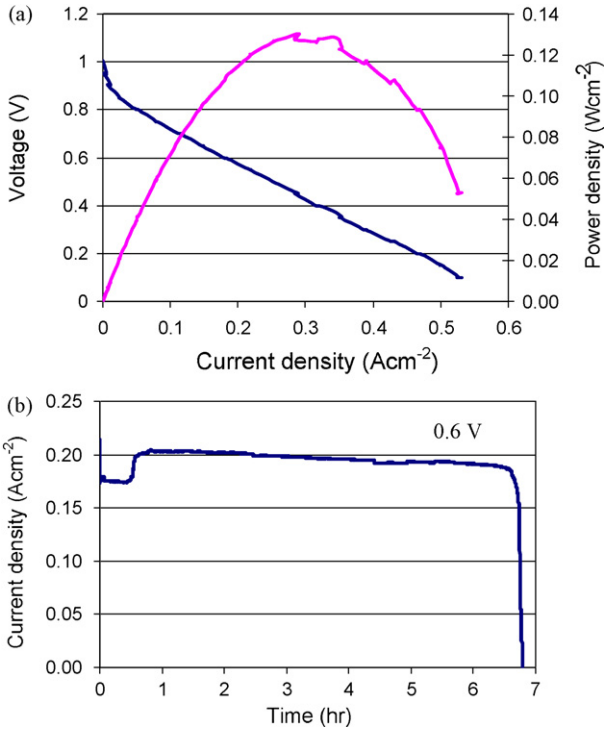

Fig. 7. (a) polarization curve and power density plot of a hybrid silicon fuel cell using the hydrogen generated from Reactor 1 with CaH_2. (b) Current density produced by the silicon fuel cell using the hydrogen generated from Reactor 1 with CaH_2 as a function of operation time.

(Micro Electromechanical System) fabrication processes. Square windows are patterned on the anode side by KOH etching while 11×11 circular windows of 100 μm diameter and 100 μm apart are patterned on the cathode side by DRIE (Deep Reactive-Ion Etching). Metal contact is made by sputtering gold. Nafion® solution is painted to fill the channels with a paintbrush. The Pt-based catalyst ink is applied on top of Nafion® via a direct painting, and the resulting catalyst loading is approximately 20 mg cm^{-2}. The polarization curve of the silicon fuel cell with hydrogen generated from Reactor 1 with CaH_2 is shown in Fig. 7a, with open cell potential above 1 V and maximum power density of 0.13 W cm^{-2}. As shown in Fig. 7b, the fuel cell ran at 0.6 V with the continuous delivery of hydrogen from Reactor 1 for more than 6 h until the reaction was complete. The low current at the beginning is due to the air trapped in the reaction vessel and connection tube.

4. Conclusion

A hydrogen generation system for micro-PEM fuel cell applications using a hydride powder packed-bed reactor was investigated. The volumetric density and byproducts volume expansion are important parameters for determining the total hydrogen yield for micro-hydrogen generators. Among the hydrolysis reactions shown in Table 1, the experiments were performed with $LiBH_4$, $LiAlH_4$, $NaAlH_4$ and CaH_2 because they have faster and more complete reactions with pure water than other hydrides, giving a higher actual hydrogen volumetric density. Two different reactors were designed and tested in this work, with volumes of 56 μL and 200 μL, respectively. Controlled amounts of water were delivered to the reactor by syringe pump and a water trap was used to measure the volume of generated hydrogen.

The experimental results show that the hydrolysis reaction of $LiBH_4$ never produced more than 50% of its theoretical yield because the products and the unreacted $LiBH_4$ can form a single solid mass that clogged the reaction vessel, thus limiting the full utilization of the hydride. The hydrolysis reaction of $NaAlH_4$ has a lower reaction rate, and it does not go to full completion when only the stoichiometric amount of water was added, because the reaction produces alkaline "slurry" that reduces the reaction rate. Both $LiAlH_4$ and CaH_2 can reach 80% yield with Reactor 1, and 90% yield with Reactor 2 with stoichiometric water added. Hydrogen yields higher than 99% were achieved within several hours after water pumping stopped. The SEM images of the byproducts of $LiAlH_4$ and CaH_2 show that the byproducts form dry solid porous materials, which allow the water and gas to flow through the packed-bed, completing the reactions. These experimental results indicated that $LiAlH_4$ and CaH_2 produced the most hydrogen per unit of reactant volume. As shown in Table 2, $LiAlH_4$ has higher actual hydrogen volumetric density than CaH_2 if the volume expansion of the byproducts is considered. Both $LiAlH_4$ and CaH_2 are the suitable hydrides for the application of micro-hydrogen generation system.

Acknowledgements

This work was supported by the Defense Advanced Research Projects Agency, under contract DST 2007-0299513-000. Any opinions, findings, and conclusions or recommendations expressed in this manuscript are those of the authors and do not necessarily reflect the views of the Defense Advanced Projects Research Agency.

References

[1] K. Cowey, K.J. Green, G.O. Mepsted, R. Reeve, Curr. Opin. Solid State Mater. Sci. 8 (2004) 367–371.
[2] S.F.J. Flipsen, J. Power Sources 162 (2006) 927–934.
[3] Z.T. Xia, S.H. Chan, J. Power Sources 152 (2005) 46–49.
[4] G. Erdler, M. Frank, M. Lehmann, H. Reinecke, C. Muller, Sens. Actuators A 132 (2006) 331–336.
[5] O.J. Adlhart, Proceedings—Power Sources Symposium, 28th, 1978, pp. 29–32.
[6] J. Yeom, R.S. Jayashree, C. Rastogi, M.A. Shannon, P.J.A. Kenis, J. Power Sources 160 (2006) 1058–1064.
[7] W.M. Yang, S.K. Chou, C. Shu, J. Power Sources 164 (2007) 549–554.
[8] T. Wang, C. Chen, J.F. Li, X.G. Zhang, B.J. Xia, X.X. Li, Chem. J. Chinese U. 25 (2004) 1928–1930.
[9] C. Wang, Z.Q. Mao, R.H. Chen, G.H. Wang, X.F. Xie, Prog. Chem. 18 (2006) 30–35.
[10] J.S. Wainright, R.F. Savinell, C.C. Liu, M. Litt, Electrochim. Acta 48 (2003) 2869–2877.
[11] T. Shimizu, T. Momma, M. Mohamedi, T. Osaka, S. Sarangapani, J. Power Sources 137 (2004) 277–283.
[12] S. Motokawa, M. Mohamedi, T. Momma, S. Shoji, T. Osaka, Electrochem. Commun. 6 (2004) 562–565.
[13] J.D. Morse, R.S. Upadhye, R.T. Graff, C. Spadaccini, H.G. Park, E.K. Hart, J. Micromech. Microeng. 17 (2007) 237–242.
[14] J.D. Morse, Int. J. Energy Res. 31 (2007) 576–602.
[15] C.W. Moore, J. Li, P.A. Kohl, J. Electrochem. Soc. 152 (2005) 1606–1612.
[16] S.M. Mitrovski, R.G. Nuzzo, Lab Chip 6 (2006) 353–361.
[17] K.B. Min, S. Tanaka, M. Esashi, J. Micromech. Microeng. 16 (2006) 505–511.
[18] X.W. Liu, C.G. Suo, Y.F. Zhang, X.L. Wang, C. Sun, L. Li, L.F. Zhang, J. Micromech. Microeng. 16 (2006) 226–232.
[19] A. Heinzel, C. Hebling, M. Muller, M. Zedda, C. Muller, J. Power Sources 105 (2002) 250–255.
[20] M. Hayase, T. Kawase, T. Hatsuzawa, Electrochem. Solid State Lett. 7 (2004) 231–234.
[21] D. Gruber, N. Ponath, J. Muller, Electrochim. Acta 51 (2005) 701–705.
[22] O.J. Adlhart, P. Rohonyi, D. Modroukas, J. Driller, ASAIO J. 43 (1997) 214–219.
[23] T. Pichonat, B. Gauthier-Manuel, J. Power Sources 154 (2006) 198–201.
[24] T. Pichonat, B. Gauthier-Manuel, Fuel Cells 6 (2006) 323–325.
[25] R.S. Jayashree, L. Gancs, E.R. Choban, A. Primak, D. Natarajan, L.J. Markoski, P.J.A. Kenis, J. Am. Chem. Soc. 127 (2005) 16758–16759.
[26] K.L. Chu, M.A. Shannon, R.I. Masel, J. Micromech. Microeng. 17 (2007) 243–249.
[27] K.L. Chu, M.A. Shannon, R.I. Masel, J. Electrochem. Soc. 153 (2006) 1562–1567.
[28] K.L. Chu, S. Gold, V. Subramanian, C. Lu, M.A. Shannon, R.I. Masel, J. Microelectromech. Syst. 15 (2006) 671–677.
[29] S. Aravamudhan, A.R.A. Rahman, S. Bhansali, Sens. Actuators A 123–24 (2005) 497–504.
[30] B.R. Flachsbart, K. Wong, J.M. Iannacone, E.N. Abante, R.L. Vlach, P.A. Rauchfuss, P.W. Bohn, J.V. Sweedler, M.A. Shannon, Lab Chip 6 (2006) 667–674.
[31] M. Ay, A. Midilli, I. Dincer, J. Power Sources 157 (2006) 104–113.
[32] Y. Kojima, Y. Kawai, H. Nakanishi, S. Matsumoto, J. Power Sources 135 (2004) 36–41.
[33] Y. Kojima, Y. Kawai, M. Kimbara, H. Nakanishi, S. Matsumoto, Int. J. Hydrogen Energy 29 (2004) 1213–1217.
[34] A. Zuttel, P. Wenger, S. Rentsch, P. Sudan, P. Mauron, C. Emmenegger, J. Power Sources 118 (2003) 1–7.
[35] V.C.Y. Kong, F.R. Foulkes, D.W. Kirk, J.T. Hinatsu, Int. J. Hydrogen Energy 24 (1999) 665–675.
[36] V.C.Y. Kong, D.W. Kirk, F.R. Foulkes, J.T. Hinatsu, Int. J. Hydrogen Energy 28 (2003) 205–214.
[37] D.R. Lide, CRC Handbook of Chemistry and Physics, in: Section 3-Physical Constants of Organic Compounds and Section 4-Properties of the Elements and Inorganic Compounds, 85th ed., Boca Raton, FL, 2004.
[38] U.S. Department of Energy, Fuel Cells and Infrastructure Technologies, Multi-Year Research, Development and Demonstration Plan: Planned program activities for 2004–2015 (2003).
[39] S.D. Richardson, T.A. Ternes, Anal. Chem. 77 (2005) 3807–3838.
[40] D. Gervasio, S. Tasic, F. Zenhausern, J. Power Sources 149 (2005) 15–21.
[41] J.C. McDonald, D.C. Duffy, J.R. Anderson, D.T. Chiu, H.K. Wu, O.J.A. Schueller, G.M. Whitesides, Electrophoresis 21 (2000) 27–40.
[42] A. Pinto, D.S. Falcao, R.A. Silva, C.M. Rangel, Int. J. Hydrogen Energy 31 (2006) 1341–1347.
[43] Y. Kojima, K. Suzuki, K. Fukumoto, Y. Kawai, M. Kimbara, H. Nakanishi, S. Matsumoto, J. Power Sources 125 (2004) 22–26.
[44] A.V. Pattekar, M.V. Kothare, J. Microelectromech. Syst. 13 (2004) 7–18.
[45] J.S. Zhang, Y. Zheng, J.P. Gore, T.S. Fisher, J. Power Sources 165 (2007) 844–853.
[46] S.C. Amendola, S.L. Sharp-Goldman, M.S. Janjua, N.C. Spencer, M.T. Kelly, P.J. Petillo, M. Binder, Int. J. Hydrogen Energy 25 (2000) 969–975.
[47] S.C. Amendola, S.L. Sharp-Goldman, M.S. Janjua, M.T. Kelly, P.J. Petillo, M. Binder, J. Power Sources 85 (2000) 186–189.
[48] R. Aiello, J.H. Sharp, M.A. Matthews, Int. J. Hydrogen Energy 24 (1999) 1123–1130.
[49] G.K. Pitcher, G.J. Kavarnos, Int. J. Hydrogen Energy 22 (1997) 575–579.
[50] V. Serebrennicov, Portable Hydrogen Power Pack, Magnic International Inc., Durham, NC, 1997.
[51] J.E. Stearns, M.A. Matthews, D.L. Reger, J.E. Collins, Int. J. Hydrogen Energy 23 (1998) 469–474.
[52] P.P. Prosini, P. Gislon, J. Power Sources 161 (2006) 290–293.
[53] M.M. Kreevoy, R.W. Jacobson, Ventron Alembic 15 (1979) 2–3.
[54] J. Huot, G. Liang, R. Schulz, J. Alloys Compd. 353 (2003) 12–15.